Physica Scripta

INCLUSIVE PUBLISHING TRUSTED SCIENCE

PURPOSE-LED PUBLISHING™

PAPER • **OPEN ACCESS**

Atomic ordered doping leads to enhanced sensitivity of phosgene gas detection in graphene nanoribbon: a quantum DFT approach

To cite this article: R Deji *et al* 2024 *Phys. Scr.* **99** 035931

View the article online for updates and enhancements.

You may also like

- Strain dependence of the heat transport properties of graphene nanoribbons
Pei Shan Emmeline Yeo, Kian Ping Loh and Chee Kwan Gan
- Effects of uniaxial strain on the performance of armchair graphene nanoribbon resonant tunneling diode
Milad Zoghi and M Z Kabir
- A DFT modulated analysis of manganese doped graphene nanoribbons as a potential material for sensing of highly toxic gases CO, PH_3 and SbH_3
Jyoti R, Moondeep Chauhan, Rajiv Kashyap et al.

This content was downloaded from IP address 160.114.157.146 on 05/05/2025 at 10:16

Physica Scripta

PAPER

Atomic ordered doping leads to enhanced sensitivity of phosgene gas detection in graphene nanoribbon: a quantum DFT approach

R Deji[1], G N Nagy[1], B C Choudhary[2], Ramesh K Sharma[3], Manish K Kashyap[4,*] and Mousumi Upadhyay Kahaly[1,*]

[1] ELI ALPS ELI-HU Non-Profit Ltd. Wolfgang Sandner utca 3, Szeged H-6728, Hungary
[2] National Institute of Technical Teachers Training & Research (NITTTR), Chandigarh –160019, India
[3] CIL/SAIF/UCIM, Panjab University, Chandigarh-160014, India
[4] Renewable Energy Laboratory, School of Physical Sciences, Jawaharlal Nehru University, New Dehli-110067, India
[*] Authors to whom any correspondence should be addressed.

E-mail: manishdft@gmail.com **and** Mousumi.UpadhyayKahaly@eli-alps.hu

Keywords: density functional theory, graphene nanoribbons, phosgene detection, first principles calculations, phosphorus doping

Supplementary material for this article is available online

OPEN ACCESS

RECEIVED
27 June 2023

REVISED
16 January 2024

ACCEPTED FOR PUBLICATION
1 February 2024

PUBLISHED
13 February 2024

Original content from this work may be used under the terms of the Creative Commons Attribution 4.0 licence.

Any further distribution of this work must maintain attribution to the author(s) and the title of the work, journal citation and DOI.

Abstract

We explore a novel sensor for detection of phosgene gas by graphene derivatives such as pristine and doped graphene nanoribbons via first principles calculations. The interaction of phosgene molecule with various edge and center doped configurations of boron, phosphorus and boron-phosphorus co-doped armchair graphene nanoribbon (AGNR) and zigzag graphene nanoribbon (ZGNR) is investigated through density functional theory (DFT). P-doped systems showcase chemisorption, displaying enhanced sensitivity to phosgene detection as reflected by a more negative adsorption energy values, accompanied by a prominent charge transfer due to the doping. Regardless of nanoribbon geometry, the binding energies of P-doped systems exhibit notable uniformity within the range of −8.01 eV to −8.49 eV, however the adsorption energies in ZGNR are significantly lower than those observed in AGNR. Due to much higher(lower) electron-donating (accepting) capacity of phosphorous(boron) atoms in comparison to 'C' atom, substitutional doping with 'P' or 'B' atoms in AGNR has signifiant impact on the structural, electronic and adsorption properties of the nanoribbons. We observe that phosphorus doped configurations (edge/center) effectively interact with phosgene molecule with higher adsorption that corresponds to the chemisorption phenomenon. The strongest adsorption energy (−8.83 eV) is obtained for P doped configurations, followed by that for B+P co-doped AGNR (−4.23 eV). These results suggest significantly stronger adsorption of phosgene gas on P doped AGNR than on any other systems reported so far. Band structure analysis estimates that by phosphorus doping, changes in the band gap is significant and it also shows prominent changes in the band structures. Isosurface electronic charge density plots identify that the transfer of charge takes place from graphene system to phosgene molecule. Thus, significant variation in adsorption and electronic properties of P doped AGNR reveal that these geometries immensely promote the detection of phosgene gas, and may be considered as promising chemical sensor for phosgene removal.

1. Introduction

Monitoring of poisonous and harmful gases such as nitrogen based gases (NO and NO_2), carbon based gases (CO and CO_2), sulphur based gases (SO, SO_2 and SO_3), hydrogen cyanide(HCN) and phosgene gas ($COCl_2$) has been a challenge for scientific society for the improvement of human health and the environment [1]. In a recent interesting work, Fadardi *et al* demonstrated the adsorption of some common hazardous gases (CO, NO, NO_2, and CO_2) on the stanene armchair nanoribbon [2]. Phosgene is a toxic and colorless gas which has been used as a

© 2024 The Author(s). Published by IOP Publishing Ltd

chemical weapon during the first world war. It is a volatile organic compound with a chemical formula of $COCl_2$ [3]. It is observed from literature that it is indeed harmful and difficult to detect. It is released during combustion of carbon tetrachloride, trichloro-ethylene and other halogenated hydrocarbons present in common materials like plastic foam. Its exposure can cause severe effects on the human health such as lung damage, blurred vision, throat and eye irritation and even cause death when inhaled at low concentration [3, 4]. Therefore, phosgene content in work environments needs to be monitored using a sensitive, and precise technology in order to be controlled in the air. Till date, various nanomaterials from nanotubes to nanopowders have been proposed as sensors [5–11]. Since, the discovery of carbon based nanomaterials such as carbon nanotubes [12, 13], fullerenes, and carbon nano cones, due to their better electric, physical [14] and mechanical properties, they are considered promising candidates for diverse applications including gas sensing [15, 16]. The adsorption and sensing of phosgene in sensor technology is still scarce. The simulation study of such a highly toxic gas help us in designing of good sensor devices.

Carbon based nanostructures, like graphene, carbon nanotubes [17], attracted more attention due to their outstanding properties, such as large surface area, high mechanical strength, and high stability [18–21]. Felegari and Hamedani [22] investigated the adsorption of phosgene molecule on γ-graphyne, BN and Si doped graphynes using DFT calculations and also studied the sensitivity of graphyne towards the phosgene adsorption. Their calculated results show that pristine and BN doped graphynes have adsorption energies (E_{ads}) of −0.11 eV and −0.21 eV which shows physical nature of adsorption but Si doped graphyne have an E_{ads} of −1.65 eV. Sc-doped BN nanotubes were used by J Beheshtian *et al* [23] for the detection of phosgene molecule. A very low value of E_{ads} of 0.06 eV indicates its poor sensitivity towards phosgene detection. Pankaj Srivastava *et al* investigated the sensing behavior of bare zigzag boron nitride nanoribbon (ZBNNR) for the toxic gas phosgene with use of DFT calculations. Their finding reveals that ZBNNR cannot be considered as good material for the sensing of phosgene due to very low value of E_{ads} of 0.08 eV [24]. Shakerzadeh *et al* [25] studied the phosgene adsorption onto pristine, Al and Ga doped boron nitride nanoclusters. According to their results, E_{ads} for pristine, Al and Ga doped boron nitride nanoclusters ranges from −0.19 eV to −0.94 eV. This indicated the physisorption nature or low adsorption ability of boron nitride nanoclusters towards phosgene detection. Baei *et al* [26] determined the sensing ability of aluminium nitride nanocage towards $COCl_2$ molecule. Their results revealed that the electronic properties of aluminium nitride nanocage are not so much sensitive towards adsorption of phosgene molecule having E_{ads} ranges from −0.13 eV to −0.59 eV. Furthermore, Zhang *et al* [27] used first-principles calculations to study sensing behavior of the phosgene molecule on undoped graphene and transition metal (TM) doped (TM = Zr, Mo, Ti, Mn, Fe, Co) graphene. They predicted that the adsorption behavior of phosgene molecule with pristine graphene is physisorption, with a very low adsorption energy of −0.55 eV. However, adsorption energies for transition metal doped graphene lies in range of −0.82 eV to −1.67 eV [28]. While doping with transition metals promotes stronger chemical adsorption of phosgene on the doped graphene surface, thereby making TM doped graphene a potential candidate for phosgene sensing, unfortunately its experimental realization is challenging [28]. Transition metal adatoms readily diffuse and demonstrate strong cluster formation tendency at room temperature [28], thereby posing technical difficulties.

Introduction of defects and dopants into carbon nanostructures are well-recognized approaches to tune their physical and chemical properties [29, 30]. Latest advanced control technology entails high-level precision in the design and synthesis of nanostructures at atomic scale, for example, through bottom-up synthesis of molecular precursors [31, 32], which indeed opens up possibilities of substitutional doping of impurity atoms into the nanoribbons in a precise location. To increase the extent of gas adsorption and chemical sensing properties, materials such as boron, phosphorus and boron phosphorous co-doped AGNR have been introduced recently [33–35]. Doping with boron and phosphorus atoms result in strong covalent type doping and the physiochemical properties of the resulting doped AGNRs are similar to that of carbon atoms. Therefore, we understand their utility in phosgene detection. The main goal of this work is to study the effect of ordered doping of heteroatoms (boron, phosphorus and boron phosphorus co-doping) on sensing behavior of graphene nanoribbons towards phosgene detection based on DFT calculations. This type of study has not been previously reported in literature to the best of our knowledge. Using first-principles study, we plan to explain adsorption behavior, charge transfer, band structures and density of states of present nanosystems.

2. Theoretical details

First-principles calculations based on DFT as implemented in ATK-VNL Toolkit [33] were performed for pristine, 'B', 'P' and 'B+P' doped graphene nanoribbons. The generalized gradient approximation (GGA) with in Perdew–Burke–Ernzerhof (PBE) parameterization [36] was used as exchange correlation functional, since it often proves to be sufficient for gas molecule adsorption, particularly chemisorption on graphene based nanoribbons [37, 38]. Norm-conserving pseudopotential [39] was considered for the present study and the

density mesh cutoff was fixed at 75 Hartree. The Brillouin zone was sampled by 100×1×1 k- mesh, corresponding to the one-dimensional periodicity of the structure along the *x* axis. The selection of such fine k-mesh, as done in a previous work [18], ensures convergence of the band gap, particularly in case of the structures that are found to be metalic. The stress and force tolerance had been selected as 0.05 eV A^{-3} and 0.05 eV Å, respectively. A fixed value of 300 K for electron temperature was used for the simulation. For graphene nanoribbon, a vacuum of 20 Å was introduced into system to avoid interactions between adjacent layers along the *z*-axis. The Vienna ab-initio simulation package (VASP) software based on DFT was used to study the charge density difference plots of various configurations for studied nano systems.

3. Results and discussion

A supercell of 3×3×1 was modelled for AGNR to study the adsorption behavior of phosgene gas on its surface. The AGNR consists of 42 carbon (C) and 12 hydrogen (H) atoms. The bond lengths of 'C–C' and 'C–H' were taken as 1.42 Å and 1.09 Å, respectively [40] and the total length of AGNR was set to be 11.36 Å. Different orderly doped AGNRs structural models passivated with hydrogen atoms were designed for the study. The number of dimer carbon atom chains across the width direction defines the width of AGNR as 'W'. The predicted values of adsorption energies listed in table 1 with W = 9 are in better agreement with earlier published work [27], therefore we considered W = 9 in the present work. AGNR was assumed to be orderly doped with a row of 'B' atoms, 'P' atoms and co-doped 'B+P' atoms along the length direction (*x* axis) of the AGNR at the edge and the center position. Various sensing systems are formed by ordered doping of boron (B), phosphorus (P) and boron phosphorus (B+P) atoms into graphene nanoribbon with 6 'C' atoms substituted by 6 'B', 6 'P' and 3'B' +3'P' atoms. All the structural models of AGNR after addition of B, P and B+P atoms along with pristine form are depicted in figure 1.

For sensing of phosgene by AGNR systems, a phosgene molecule is placed initially at a distance <3 Å from graphene nanoribbon and the full system is allowed to relax to minimize the forces and energies. Phosgene ($COCl_2$) is a planar molecule with C=O (d_3) distance as 1.18 Å, the C−Cl (d_1 and d_2) distances as 1.74 Å and the Cl−C−Cl bond angle as 111.8° [4] (see figure 1(h)). H, O, C, B, P and Cl atoms are shown by white, red, brown, green, orange and purple color spheres in figure 1.

3.1. Stability analysis and Binding energy calculations

Firstly, we studied the stability of all nano systems considered in present work. The stability of various configurations is evaluated by calculation of binding energies (E_b). Furthermore, binding energies (E_b) of dopant atoms are calculated by using equation (1) [41].

$$E_b = \frac{1}{t}[E_T - (pE_C + qE_H + rE_P + sE_B)] \quad (1)$$

Here, t represents the total number of atoms, E_T represents the total energy of structure, and E_C, E_H, E_B, and E_P represents the isolated energy of C, H, B, and P atoms, respectively. Further, p, q, r, and s represent the total number of C, H, P and B atoms, in one modeled unit cell, respectively

Figure 1 shows the front view of atomic structures formed after doping with 6B, 6 P and 3B+3 P atoms into the graphene domain and corresponding configurations are formed: B edge AGNR, B center AGNR, P edge AGNR, P center AGNR, BP edge AGNR and BP center AGNR. The schematics for all studied nanosystems before and after relaxations are given in figure 1.

As shown in figure 1(a), after relaxation, negligible changes are seen in optimized geometries of pristine AGNR. In case of 'B' doped geometries, changes are minimal in optimized geometries as compared to other doped geometries as shown in figures 1(b)–(c). As in figure 1(d), in case of P edge AGNR, after optimization the bond between 'P' and 'H' is broken due to weak vander Waals forces of attraction and in P center AGNR (figure 1(e)), the repulsions between phosphorus atoms take place due to large atomic size of phosphorus atoms as compared to carbon atoms. On the other hand, in 'B+P' co-doped geometries (figures 1(f), (g)), boron and phosphorus atoms are little bit protruded from their plane as compared to phosphorus doped variants. The binding energies of various configurations follow the order: P edge AGNR (−8.11 eV) > P center AGNR (8.01 eV)> BP edge AGNR (−7.19 eV) > BP center AGNR (−7.17 eV) > B edge AGNR (−7.15 eV) > B center AGNR (−7.14 eV).

As summarized in table 1, the binding energies of 'P' doped geometries among the considered ones are the highest among all variants as phosphorus atoms are strongly interacting with graphene nanoribbons and distortion in these systems is minimal. However, the width of the nanoribbon, as well as the location of the dopant atoms in the lattice, may also play a role. In order to investigate this effect, we have investigated the adsorption energetics in two additional geometries with different nanoribbon width (n) in the P-doped case: P edge AGNR with a ribbon width of 5 graphene hexagons (n = 5), and P center AGNR with a ribbon width of 4

Table 1. Adsorption energies of all studied configurations (in eV), binding distance, bond lengths and bond angles after adsorption of $COCl_2$, binding energies(eV).

Sr No.	Variants	Eads (adsorption energy) (in eV)	Binding distance (in Å)	Bond lengths after adsorption (in Å)			Bond angle after adsorption (Cl-C-Cl)	Binding Energy (eV)
				d1 (C-Cl)	d_2 (C-Cl)	d3 (C=O)		
1.	Pr edge AGNR	−0.65	3.56	1.75	1.74	1.19	110°	—
2.	Pr center AGNR	−0.65	3.47	1.74	1.74	1.19	110°	—
3.	B edge AGNR	−4.43	2.87	1.73	1.78	1.19	109°	−7.15
4.	B center AGNR	−1.76	2.94	1.74	1.79	1.19	110°	−7.14
5.	BP edge AGNR	−4.23	3.81	1.74	1.74	1.19	111°	−7.19
6.	BP center AGNR	−3.65	3.47	1.74	1.75	1.19	110°	−7.17
7.	P edge AGNR (n=3)	−8.83	2.60	1.74	1.74	1.20	111°	−8.11
8.	P center AGNR (n = 3)	−7.46	2.22	1.77	1.74	1.20	111°	−8.01
9.	P edge AGNR (n = 5)	−12.208	2.02	1.73	1.71	1.19	112 °	−8.42
10.	P center AGNR (n = 4)	−9.820	2.31	1.71	1.71	1.20	113°	−8.23
11.	P_2 edge ZGNR (n = 3)	−4.301	2.58	1.72	1.72	1.19	112°	−8.35
12.	P_2 edge ZGNR (n = 4)	−4.272	2.36	1.73	1.71	1.19	111°	−8.49
13.	P_2 center ZGNR (n = 3)	−5.927	2.00	1.74	1.70	1.19	111°	−8.32
14.	P_2 center ZGNR (n = 4)	−6.486	1.97	1.73	1.71	1.19	112°	−8.46

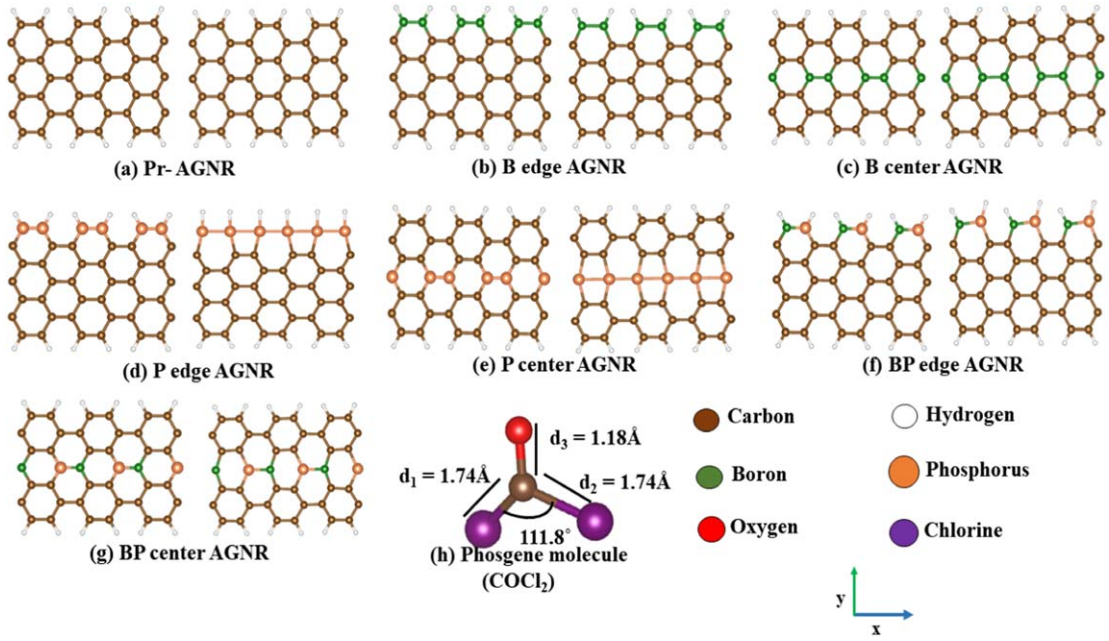

Figure 1. Front view of initial and relaxed (optimized) geometries of all configurations before phosgene adsorption; (a) Pr-AGNR, (b) B edge AGNR, (c) B center AGNR, (d) P edge AGNR, (e) P center AGNR, (f) BP edge AGNR, (g) BP center AGNR, (h) Phosgene molecule ($COCl_2$).

graphene hexagons. These are shown on figures 2(e)–(h). Furthermore, four structures with similar doped graphene nanoribbons in zigzag geometry (ZGNR) are investigated to determine the effect of the crystallographic orientation of the nanoribbon. However, in these cases, only a local doping with two neighboring P atoms is used due to the close distance of neighboring lattice sites in the periodic direction, which causes an increased strain in the P-P bonds in the relaxed structure. The corresponding structures: P2 center ZGNR (n = 3 and n = 4) (figures 2(i)–(l)), and P2 edge (n = 3 and n = 4) (figures 2(m)–(p)). As shown in table 1, we can observe that the binding energies are all similar for the P-doped systems (between −8.01 eV and −8.49 eV) regardless of the nanoribbon geometry, with a slight negative increase with an increasing width of the nanoribbon in both the armchair and zigzag cases. Furthermore, the adsorption energies in the ZGNR case are significantly lower than in the AGNR case, varying between −4.3 eV and −6.4 eV. Correspondingly, we can conclude that the adsorption process is more favorable in the AGNR case, and the adsorption mechanism is not affected significantly by the width of the nanoribbon. As such, in the following, we keep the focus of this manuscript to the AGNR geometry with a width of n = 3 hexagons.

Gas sensing mechanism works in two ways: Physisorption and Chemisorption. Physisorption corresponds to weak van der Waals forces of attraction between gas molecule and substrate [42]. The physisorption of molecules onto the nanoribbon substrate has been explored in the work of Fadardi *et al* [2], where they studied the adsorption of various common hazardous gases, including CO, NO, NO_2, and CO_2, on the stanene armchair nanoribbon. This process was found to have a less negative value of adsorption energy. Less charge gets transfer between phosgene molecule and graphene system in physisorption. Chemisorption represents strong chemical bonding between the gas molecule and the substrate and also has more negative value of adsorption energy. The whole adsorption phenomenon can be better understood in terms of range of energy of adsorption. Physisorption falls in the energy range of the order of 10^{-2} eV and for chemical type of bonding (sharing of electrons between gas and target material), adsorption energies are always greater than 1 eV or more [43]. Larger values of E_{ads} greater than 1 eV particularly indicate chemical bond formation. On the other hand, more charge will be transferred between graphene and phosgene molecule. The adsorption energies (E_{ads}) define the extent of interaction between the phosgene molecule and pristine or doped graphene nanoribbons, calculated by the following equation [44].

$$E_{ads} = E_{AGNR+GAS} - (E_{AGNR} + E_{GAS}) \quad (2)$$

where, $E_{AGNR} = E_{doped/\ undoped}$ AGNR represents the total energy of doped/ undoped AGNR, $E_{AGNR+GAS} = E_{doped/\ undoped\ AGNR\ +\ phosgene}$ gives the same type of energy after adsorption of phosgene, and $E_{GAS} = E_{phosgene}$ represents the energy of phosgene molecule, respectively.

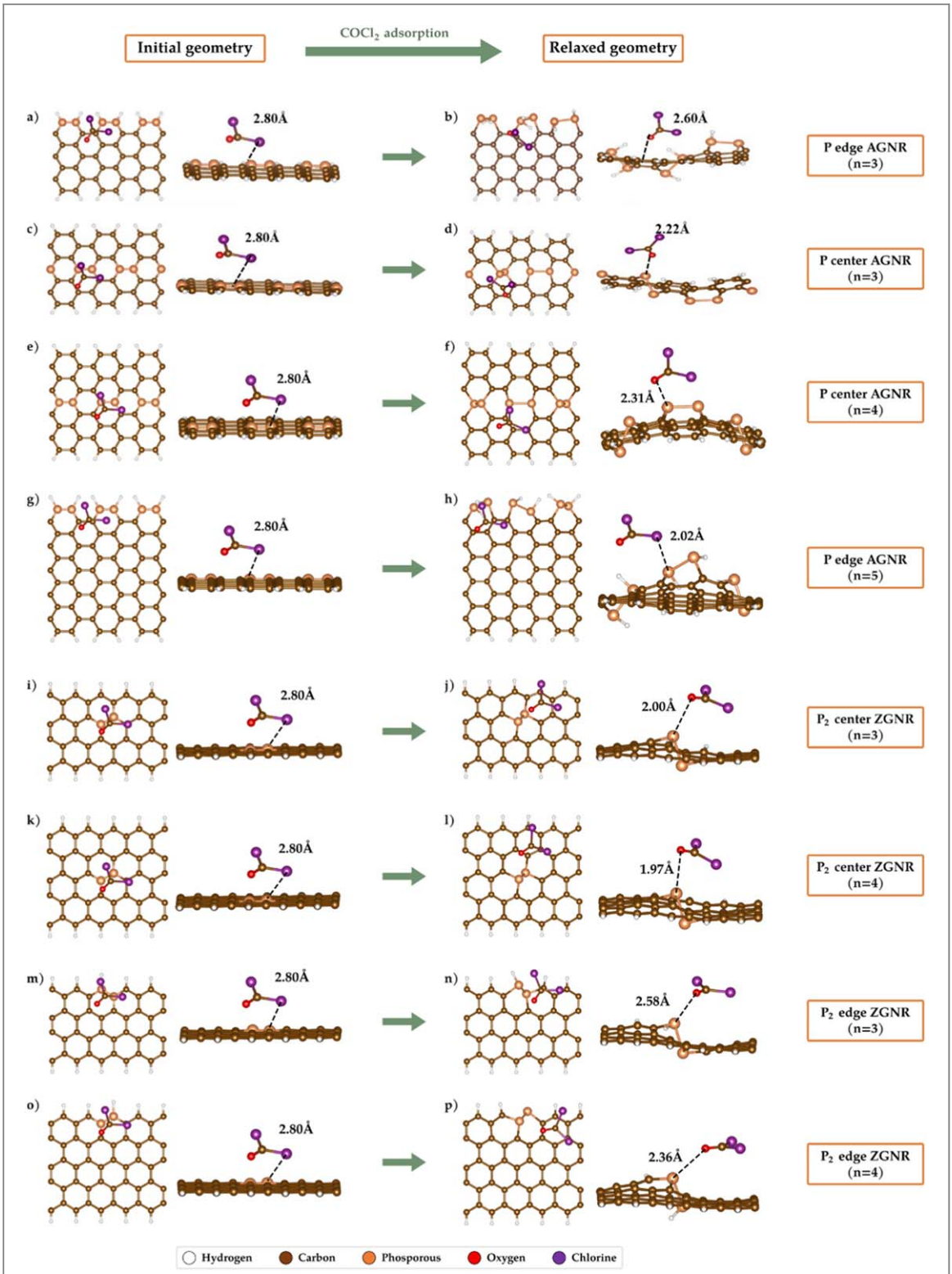

Figure 2. Front and side views of the initial and relaxed geometries for different configurations of P-doped graphene nanoribbons after adsorption of a phosgene molecule, with varying width (n) and edge orientation. Binding distances are illustrated for each configuration. (a)-(b) P edge AGNR (n = 3); (c)-(d) P center AGNR (n = 3); (e)-(f) P center AGNR (n = 4); (g)-(h) P edge AGNR (n = 5) in armchair orientation; and (i)-(j) P_2 center ZGNR (n = 3); (k)-(l) P_2 center ZGNR (n = 4); (m)-(n) P_2 edge ZGNR (n = 3); (o)-(p) P_2 edge ZGNR (n = 4) in zigzag orientation.

3.2. Geometric parameters and Adsorption energy of all doped systems

For detection of phosgene, pristine AGNR and 6 possible geometries with a ribbon width of 3 hexagons were considered to find out the most favorable geometry for adsorption. These adsorption geometries are shown on figure S1 and S2, and 'C' atom in pristine, 'B' atom in B edge AGNR, B center AGNR, BP edge AGNR and BP center AGNR were considered as active adsorption site due to accumulation of local positive charge around it

and 'P' atom in P edge AGNR and P center AGNR was taken as active site for adsorption. All calculated parameters such as adsorption energies, binding distance, changes in bond lengths and bond angles after adsorption are listed in table 1 for these systems as well as the P-doped systems in different nanoribbon geometries. The binding distance is the closest distance of 'Cl' atom of phosgene molecule with doped (B, P) atom of AGNR. As shown in figure S1, phosgene molecule was placed parallel to Pr edge AGNR with chlorine ('Cl') atom of phosgene molecule facing towards graphene nanoribbons. Initially, phosgene molecule ($COCl_2$) with 'Cl' atom of phosgene interacts with 'C' atom at edge in figures S1(a)–(b) and at center position in figures S1(c)–(d), after adsorption, the orientation of phosgene molecule was parallel to graphene nanoribbon and no significant changes were observed in optimized geometry of Pr edge AGNR and Pr center AGNR. However, after adsorption of phosgene molecule with pristine system at both edge and center position, 'Cl' atom moved away from pristine graphene system. After interaction, 'Cl' atom of phosgene molecule in case of Pr edge AGNR, stabilized itself at a distance of 3.56 Å (figure S1(b)) and in case of Pr center AGNR, it get relaxed at a distance of 3.47 Å (figure S1(d)). The bond lengths and bond angle of phosgene molecule after interaction with Pr-AGNR at edge position were found to be d_1 (C-Cl) = 1.75 Å, d_2 (C-Cl) =1.74 Å, d_3 (C=O) =1.19 Å, Cl- C-Cl = 110° and at center position, these were d_1 (C-Cl) = 1.74 Å, d_2 (C-Cl) =1.74 Å, d_3 (C=O) = 1.19 Å, Cl- C-Cl = 110°, respectively. These minimal changes in bond lengths and bond angle of phosgene molecule suggests that the molecule remains intact even after its interaction with pristine surface. The adsorption of phosgene onto Pr-AGNR at edge and center position resulted into weak interaction with an adsorption energy (E_{ads}) of −0.65 eV. This indicates weak adsorption (van der Waals forces of attraction) and reveals physical nature of interaction. After adsorption of $COCl_2$, negligible changes in optimized geometries of Pr edge AGNR and Pr center AGNR were observed. In order to consider the interaction of $COCl_2$ with 'B' doped graphene geometries, the phosgene molecule with its 'Cl' atom was placed parallel to 'B' doped configurations (figures S1 and S2).

After adsorption of phosgene, phosgene was relaxed on the 'B' atom with its 'Cl' atom head at a distance of 2.87 Å /2.94 Å (figures S1(f), S2(h)) for B edge AGNR /B center AGNR. After adsorption, bulges or protruding type changes were seen in their optimized geometries (see figures (S1(f), S2(h)) with adsorption energy values as −4.43 eV (B edge AGNR) and −1.76 eV (B center AGNR). The size of boron atom is very small or comparable to carbon atom, thus boron atoms were minorily pulled out from graphene nanoribbon surface. The changes produced in the optimized geometries and larger adsorption energies of B doped geometries indicate the chemisorption nature of adsorption as compared to pristine surface. Here, it is important to note that van der Waals interactions can play a pivotal role in influencing binding energies and site preferences, especially in scenarios where the physisorption of molecules onto the adsorbent takes place. However as we observe that phosphorus doped configurations (edge/center) effectively interact with phosgene molecule showing high adsorption energy that corresponds to the chemisorption phenomenon. The bond lengths and charge transfer, as will be discussed later, also indicate chemisorption. Therefore, for our systems, integrating van der Waals (vdW) calculations is anticipated to result in only marginal alterations, while the trends are expected to remain same/similar. Thus, for phosgene sensing, we use GGA exchange correlation, which proves sufficient to capture the trends and is previously adopted in many previous works for gas molecule adsorption on graphene nanoribbons [37, 38, 42]. The changes in bond lengths and bond angle of phosgene molecule after interaction with B doped edge position were d_1 (C-Cl) = 1.73 Å, d_2 (C-Cl) =1.78 Å, d_3 (C=O) = 1.19 Å, Cl- C-Cl = 109° and at B doped center position, these were d1 (C-Cl) = 1.74 Å, d2 (C-Cl) =1.79 Å, d_3 (C=O) =1.19 Å, Cl- C-Cl = 110°. Similar observation of slight increase of bond lengths in adsorbed gas molecule has been previously reported by other researchers [42], indicating possible 'expansion of gas molecule' post adsorption. Thus, geometrical changes in phosgene molecule are significant after its interaction with 'B' doped geometries as compared to pristine surface.

In P edge AGNR and P center AGNR, initially, 'Cl' atom was facing towards 'P' atom at the edge and the center position (figures 2(a), (c)). After interaction with $COCl_2$, 'P' atoms were pulled out from nanoribbon and 'O' atom of $COCl_2$ came closer to 'P' atom with a binding distance of 2.60 Å (figure (2(b)). On the other hand, when the phosgene molecule with its 'Cl' end interacts with the P center AGNR, the 'O' atom moved closer to 'P' atom with a binding distance of 2.22 Å (figure (2(d)). In P doped geometries, we observed that after adsorption of phosgene, all phosphorus atoms were found on the above of graphene plane instead of embedding into graphene nanoribbon which may be due to larger atomic radius of 'P' atom than that of 'C' atom. This significant difference in atomic radius of 'C' and 'P' atoms produced strain in graphene nanoribbon and phosphorus atoms were lifted from their positions figures (2(b), (d)). The adsorption of phosgene resulted into more bulges or protruding type structures as compared to other geometries. As shown in table 1, E_{ads} between phosgene and P edge AGNR /P center AGNR were found to be −8.83 eV/ −7.46 eV, respectively. Therefore, 'P' doping strengthened the adsorption of phosgene molecule significantly and resulting into better sensitivity of the graphene nanoribbon. The elevations that appeared in case of phosphorus doped structures were caused by the difference between atomic radius of 'C' atom and 'P' atom. The calculated value of bond lengths and bond angle of phosgene molecule after adsorption with P edge AGNR were d_1 (C-Cl) = 1.74 Å, d_2 (C-Cl) = 1.74 Å, d_3

(C=O) = 1.20 Å, Cl- C-Cl = 111° and with P center AGNR, these were d_1 (C-Cl) = 1.77 Å, d_2 (C-Cl) =1.74 Å, d_3 (C=O) = 1.20 Å, Cl- C-Cl = 111°. Regarding the geometry of the adsorption, similar results are observed in case of the increased nanoribbon width (figures 2(e)–(h)), with further increased adsorption energies. The high adsorption energy and small binding distance in case of P-doped AGNR indicates that there is strong interaction occurring between phosgene and P doped configurations owning to chemisorption which leads to chemical bond formation. In case of the ZGNR geometry, we can observe a significant buckling at the location of doping, caused by the increased strain introduced by the P-P bond, causing a significant buckling. As in the armchair case, the O atom of the phosgene molecule tends to beclosest to the P atoms, with a similar adsorption distance. However, the adsorption energy is reduced, suggesting a decrease in the strength of the chemical nature of the bonding.

P center AGNR (n = 4); (g)-(h) P edge AGNR (n = 5) in armchair orientation; and (i)-(j) P_2 center ZGNR (n = 3); (k)-(l) P_2 center ZGNR (n = 4); (m)-(n) P_2 edge ZGNR (n = 3); (o)-(p) P_2 edge ZGNR (n = 4) in zigzag orientation

The equal amount of acceptor (boron) and donor (phosphorus) impurities introduced into the graphene nanoribbon yielded the formation of BP edge /center AGNR. We observed that 'Cl' atom of phosgene molecule got adsorbed on BP edge AGNR and BP center AGNR with adsorption energies are −4.23 eV and −3.65 eV, respectively (table 1). The interaction of phosgene with BP doped configurations also results into the strongest type of chemical adsorption.After full structural relaxation, 'Cl' atom stabilized itself at a distance of 3.81 Å/ 3.47 Å (figures S2(j), S2(l)) for BP edge /center AGNR. Less elevated structures were obtained after interaction in BP doped configurations as compared to P doped geometries. The bond lengths and bond angle of phosgene molecule after adsorption with BP edge AGNR were found to be d_1 (C-Cl) = 1.74 Å, d_2 (C-Cl) = 1.74 Å, d_3 (C=O) = 1.19 Å, Cl- C-Cl = 111° and with BP center AGNR, these were d_1 (C-Cl) = 1.74 Å, d_2 (C-Cl) =1.75 Å, d_3 (C=O) = 1.19 Å, Cl- C-Cl = 110°. It worths noting that our results of adsorption energies for B/P/B+P doped AGNR lie in range of −1.76 eV to −8.83 eV which are higher than that previously reported results for phosgene detection in systems such as Nb- doped arsenene (E_{ads} ranges from −0.21 eV to −2.90 eV) [45] and Ti, Ni and Cu decorated borospherene (E_{ads} ranges from −0.06 eV to −1.31 eV) [46], suggesting enhanced stability of the gas-solid adsorption complex, when B/P/B+P doped AGNR are used for sensing.

On the basis of higher adsorption energies, the edge doped configurations were predicted to be more energetically favorable. However, our results revealed that ordered doping is a better way to improve the adsorption of phosgene molecule and it fairly enhanced the adsorption energies to greater extent. The calculated results of adsorption energy established that 'P' doping in graphene domain is one of the prominent way for the detection of phosgene molecule. Thus, this new idea of ordered doping of acceptor and donor impurities (boron, phosphorus and boron-phosphorus) into graphene domain demonstrates the potential applicability of these materials towards phosgene detection. The P- case is most suitable for phosgene adsorption. Therefore, we will focus mainly on P- case thoroughly and discussed all the electronic properties for this case only. However, for completeness, the other cases have also been summarized in supplementary information (SI).

3.3. Density of state analysis (DOS)

To have a better understanding of the adsorption phenomenon and to figure the effect of doping of B and P atoms on the electronic properties of graphene system, density of states(DOS) has been calculated. From the DOS analysis in figure 3, we observed that before adsorption of $COCl_2$, broad peaks are observed which is denoted by orange lines and after adsorption, peaks are shown by brown lines. In figure, fermi level (E_F) is observed at 0 eV.

3.3.1. DOS of pristine AGNR

The DOS of Pr edge AGNR indicates that after the interaction of phosgene with Pr edge AGNR (figure 3(a)), peaks are observed around −2.4 eV, −2.9 eV, −3.8 eV in the valence band 'VB' (left to fermi level) and 1.8 eV in the conduction band 'CB' (right to fermi level) having corresponding DOS values are 90 eV^{-1}, 52 eV^{-1}, 51 eV^{-1} and 120 eV^{-1}. While in case of Pr center AGNR (figure 3(b)), however, peaks are seen at around −2.3 eV, −2.9 eV, −3.8 eV in VB and 2.8 eV in CB having corresponding DOS values are 85eV^{1}, 80 eV^{-1}, 70 eV^{-1} and 25 eV^{-1}. After adsorption of $COCl_2$, a little change was observed in DOS peaks around fermi level (E_F) for pristine AGNR at both edge and center position. From DOS analysis, we found that only Cl-3p states participate in DOS with C-2p states.The electronic properties of the pristine system are not greatly affected by adsorption (figures 3(a), (b)).

3.3.2. DOS of B edge / B center AGNR

The DOS plots for B edge / B center AGNR configurations are shown in figure S3. In case of B edge AGNR (figure S3(a)), DOS peaks are at around −3.9 eV, −3.8 eV, −1.7 eV, −1.5 eV in VB and 0.4 eV, 2.9 eV in CB

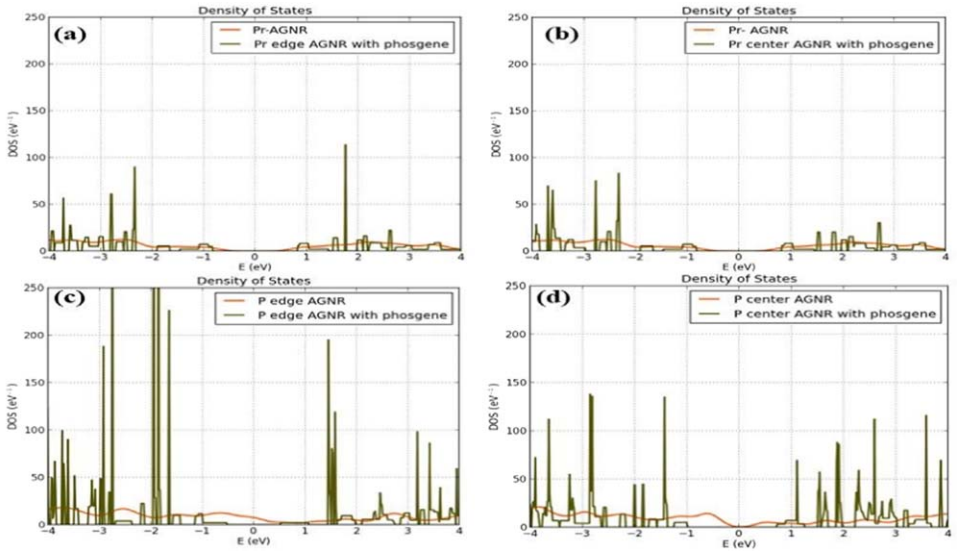

Figure 3. The DOS plots of (a) Pr edge AGNR; (b) Pr center AGNR; (c)P edge AGNR; (d) P center AGNR before and after adsorption of phosgene.

having corresponding DOS values are 148 eV^{-1}, 110 eV^{-1}, 60 eV^{-1}, 75 eV^{-1} and 70 eV^{-1}, 65 eV^{-1}. Interaction of $COCl_2$ with B center AGNR (figure S3(b)), results into DOS peaks nearer to −1.7 eV in VB and 2.5 eV in CB having corresponding DOS values are 85 eV^{-1} and 100 eV^{-1}. Thus, less intense peaks are observed in case of 'B' doped geometries. The DOS peaks are mainly contributed by '2p' electrons of B' atoms and '3p' electrons of 'Cl' atom.

3.3.3. DOS of BP edge / BP center AGNR

For adsorption of phosgene on BP edge AGNR (figure S3(c)), the corresponding DOS peaks observed at −4 eV, −3 eV, −2.5 eV in VB and 1.2 eV, 1.4 eV, 2 eV, 2.5 eV in CB having DOS values are 160 eV^{-1}, 180 eV^{-1}, 250 eV^{-1}, and 55 eV^{-1}, 200 eV^{-1}, 250 eV^{-1},250 eV^{-1}.While, for BP center AGNR (figure S3(d), DOS peaks appear at −3.5 eV, −3 eV in VB and 2 eV, 3.5 eV in CB having DOS values are 70 eV^{-1}, 100 eV^{-1} and 180 eV^{-1}, 105 eV^{-1}. Contribution to the DOS peaks comes from interaction of '3p' electrons of 'Cl' and ''2p' electrons of 'B' atom of BP edge and BP center configurations.

3.3.4. DOS of P edge / P center AGNR

The phosphorus 'P' atom significantly influences the electronic properties of AGNR and results in the modification of total DOS for both configurations such as P edge AGNR and P center AGNR. The DOS analysis of both systems (figures 3(c), (d)) reflects very sharp and more intense peaks around E_F after the adsorption of phosgene. These sharp and intense DOS peaks for both cases are caused by hybridization between P-3p states and Cl-3p states of the phosgene molecule. In case of P edge AGNR (figure 3(c)), DOS peaks are observed nearer to −3.9 eV, −3.8 eV, −3.7 eV, −3 eV, −2.9 eV, −2 eV, −1.9 eV in VB and 1.5 eV, 3.2 eV, 3.4 eV in CB having corresponding DOS values are 65 eV^{-1}, 100 eV^{-1}, 90 eV^{-1}, 187 eV^{-1}, 250 eV^{-1}, 250 eV^{-1}, 230 eV^{-1} and 190 eV^{-1}, 100 eV^{-1}, 85 eV^{-1}. On the other hand, P center AGNR (figure 3(d)), shows DOS peaks nearer to −3.8 eV, −2.9 eV, −1.5 eV in VB and 1.1 eV, 1.9 eV, 2.6 eV, 3.8 eV in CB with DOS values are 115 eV^{-1}, 140 eV^{-1}, 140 eV^{-1} and 60 eV^{-1}, 90 eV^{-1}, 110 eV^{-1}, 115 eV^{-1}, respectively. The DOS peaks confirm that these systems can be considered as good adsorbing materials for phosgene detection. The significant difference between the DOS of pristine and 'P' doped AGNR is due to the higher electronegativity of the 'P' atom than that of 'C' atom.

3.4. Band structure analysis

To get more insights into the adsorption of phosgene molecule onto doped graphene nanoribbons, the band structures were analyzed. After the adsorption of gas molecule, the delocalization of orbitals and charge transfer take place, which result into changes in the electronic structure of materials, making them suitable for gas sensing applications. The electrical conductivity (σ) of different built-in materials can be easily determined by the band gap equation (3) [47] which is as follows

$$\sigma = \exp\left(-\frac{\Delta E_g}{2k_B T}\right) \tag{3}$$

where, k_B is the Boltzmann constant and T is the temperature. The band gap values before and after adsorption of phosgene molecule and the change in band gap value (ΔE_g) are listed in table S1. Also, in figure 5, the adsorption energies (panel a) after phosgene molecule adsorption and resulting change of band gap (panel b) are represented. To further study the effect of phosgene molecule adsorption on the electronic properties of undoped and doped AGNR, band gap change (ΔE_g) was calculated for all the adsorption configurations. According to equation (3), change in band gap after adsorption of gas molecule changes the conductivity of system that corresponds to change in sensitivity of particular system. The band gap of pristine AGNR is 1.73 eV (direct band gap semiconductor) and when phosgene molecule is adsorbed on it at edge position, the band gap changes to 1.64 eV (direct band gap semiconductor) as shown in (figures S4(a)–(b)). The adsorption of phosgene molecule on pristine AGNR at center position, changes the band gap to 1.66 eV (direct band gap semiconductor) (figures S4(c)–(d)). After the phosgene molecule adsorption, band gap change (ΔE_g) is very small for Pr edge AGNR, Pr center AGNR (0.09 eV, 0.07 eV). Thus in case of pristine, after adsorption of phosgene at both edge and center position, change in band gap is not significant. This indicates that undoped AGNR cannot be considered as active material for detection of phosgene molecule.

3.4.1. B edge and B center AGNR

The doping of boron ('B') in pristine AGNR at edge and center position indicates its semi- metallic behavior. B edge AGNR configuration acquires a band gap (E_g) of 0.08 eV (direct band gap) and after adsorption, it opens the band gap to 0.72 eV (direct band gap) (figure S5(a)–(b)). In case of B center AGNR, the boron atom act as a p-type dopant shifting the fermi level in AGNR nearer to valence band than conduction band. The band gap of B center AGNR changes slightly i.e. from 0.02 eV (indirect band gap) to 0.25 eV (indirect band gap) (figure S5(c)–(d)). Since, the band gap change (ΔE_g) are 0.64 eV and 0.23 eV for B edge AGNR and B center AGNR. A small change in energy gap is observed for B doped geometries.

3.4.2. BP edge and BP center AGNR

When equal number of 'B' and 'P'atoms are added into the graphene system in a ordered way, for system BP edge AGNR, it acquires energy gap of 1.32 eV with a direct band gap and after adsorption, this changes to 0.96 eV (direct band gap material) (figure S5(e)–(f)). i.e. fine tunability of energy gap appears after detection of phosgene molecule. The BP center AGNR system attains a band gap of 1.42 eV (direct band gap semiconductor) and after interaction with $COCl_2$, the band gap changes to 1.30 eV (direct band gap semiconductor) (figure S5(g)–(h). The band gap change (ΔE_g) are 0.36 eV and 0.12 eV for BP edge AGNR and BP center AGNR which is very small. This small change in the band gap for BP doped geometries indicates that these materials cannot be considered as good material for detection of phosgene molecule although these variants have more value of adsorption energies.

3.4.3. P edge and P center AGNR

The doping of 'P' atoms in pristine AGNR at edge and center position indicates metallic and semi metallic behavior before adsorption of phosgene molecule. In case of P edge AGNR, the band gap behavior changes from metallic to semiconducting type (1.06 eV) i.e. direct band gap semiconductor (figures 4(a)–(b)). On the other hand, for P center AGNR, the band gap changes from 0.88 eV (semi-metallic) to 1.71 eV (direct band gap semiconductor) (figures 4(c)–(d)). After phosgene adsorption, opening of band gap takes place in case of P doped geometries. The band gap change (ΔE_g) is 1.06 eV and 0.83 eV for P edge AGNR and P center AGNR as shown in table S1. Thus, large band gap changes are observed for P doped configurations that results into creation of new energy states in valence and conduction bands of 'P' doped AGNR. Such prominent increase of band gap due to phosgene molecule adsorption was observed also on Carbon nanotubes and Boron Nitride nanotubes [48], indicating possibility of modulation of the electrical properties of the phosgene-adsorbent system. This large change in band gap is due to more negative value of E_{ads} that lies in chemisorption region. Thus, we can conclude that 'P' doped systems may be considered as promising materials in phosgene detection due to large band gap change, providing electric signals and having large negative value of adsorption energies among all other configurations.

3.5. Charge transfer analysis

In order to examine the phosgene adsorption capability of pristine and different doped configurations, the charge density difference images were analyzed. The charge transfer between the phosgene molecule and different variants were analyzed by Mulliken atomic charge analysis [49]. With the use of Mulliken population, the charge transfer was calculated by using the following equation:

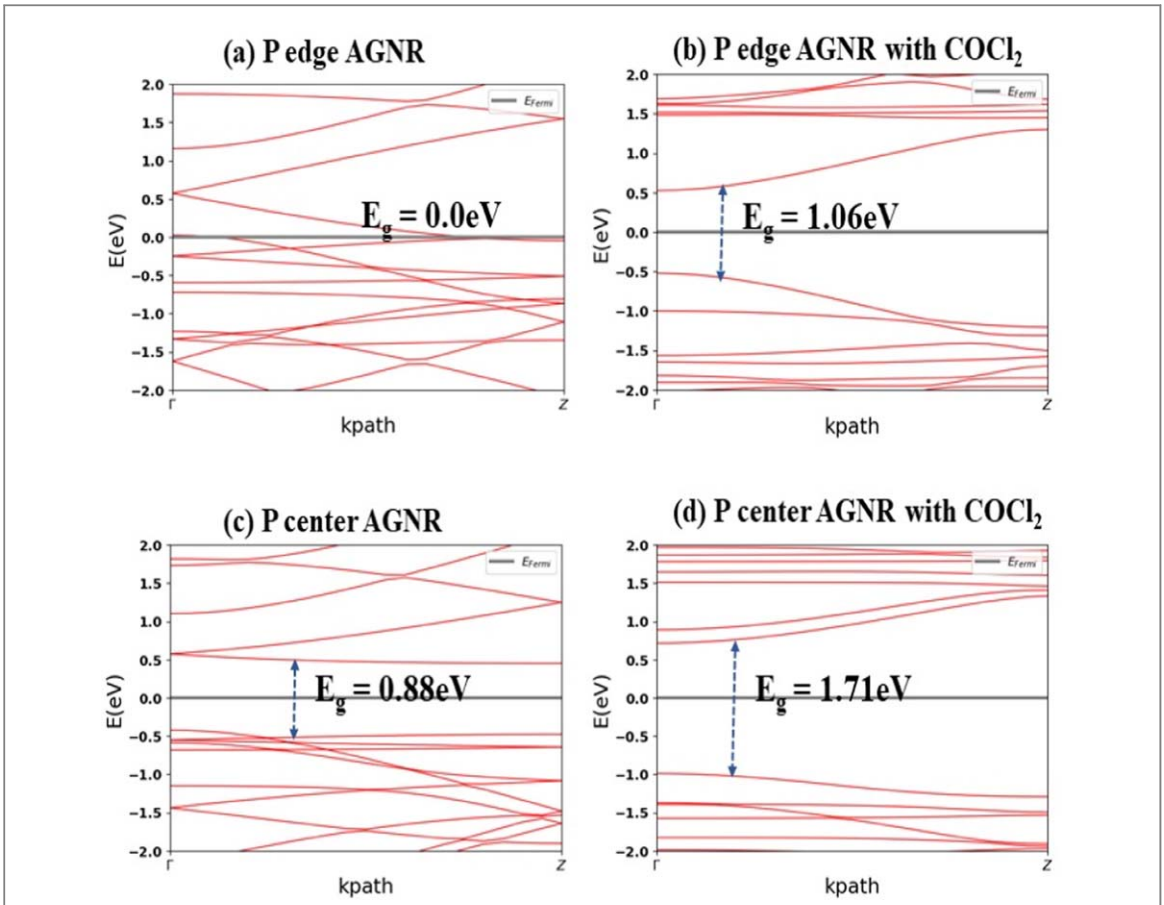

Figure 4. Band structures of (a)-(b) P edge AGNR; (c)-(d) P center AGNR.

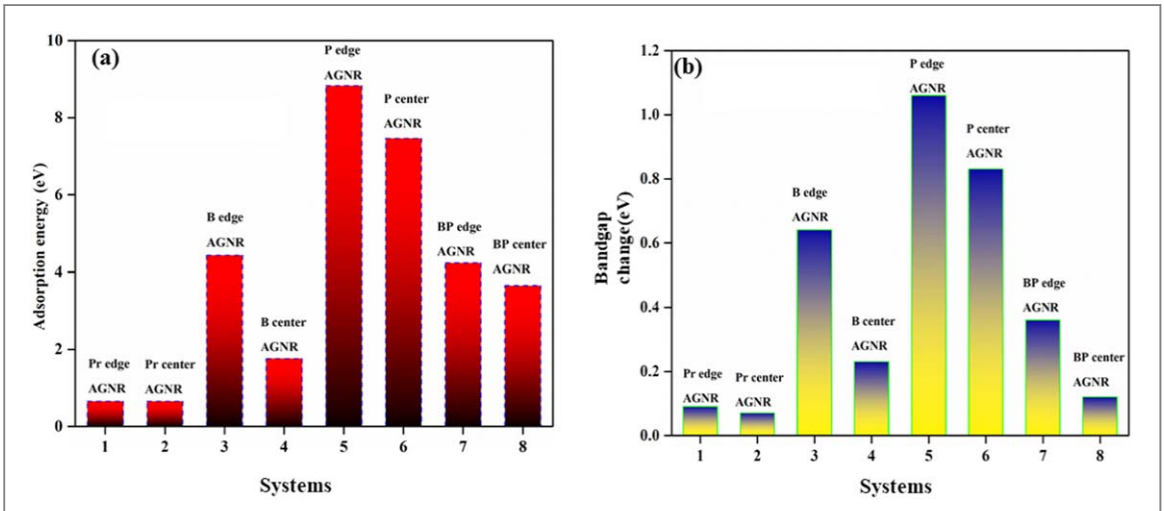

Figure 5. Bar diagram of (a) adsorption energies and (b) change of band gap (eV) before and after phosgene adsorption for all variants.

$$\Delta Q = Q_a - Q_b \tag{4}$$

where ΔQ, Q_a and Q_b indicate charge transfer between phosgene gas and different variants, Mulliken charges of the gas after and before the adsorption, respectively. The values of the charge transfer are listed in the table S1.

When the phosgene molecule interacts with pristine and doped (B/P/B+P) AGNR, a significant charge gets transferred from the graphene nanoribbons to the phosgene. A parallel observation of significant charge transfer from the nanoribbon to phosgene occurred when the phosphorene nanosheet was subjected to phosgene gas molecules [50]. This reinforces our finding that the COCl2 gas molecule functions as a potent acceptor due to its oxidizing nature with respect to P doped graphene nanoribbons, resulting in electron transitions from the P

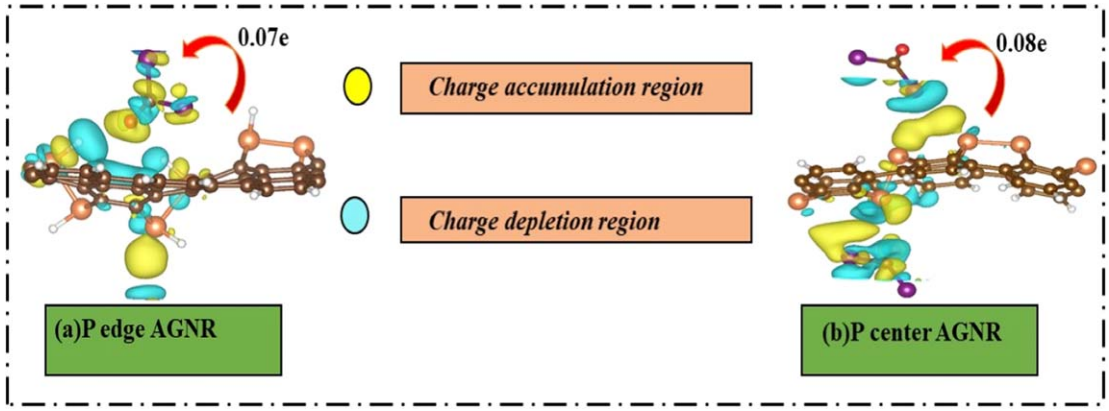

Figure 6. 3D isosurface of charge density difference with the isosurface value of 0.0003 e $Å^{-3}$ for (a) P edge AGNR, (b) P center AGNR after adsorption of phosgene ($COCl_2$).

atoms in the phosphorene nanosheet to the COCl2 gas. Here, phosgene molecule acts as a electron acceptor as shown in figure 6, where, it is surrounded by yellow region (charge accumulation region) which shows the gain of charge in the adsorption process. On the other hand, 'C' atoms in pristine AGNR and doped atoms (B and P) in doped AGNR are surrounded by cyan region (charge depletion region) which indicates the loss of charge. It is observed that the phosgene molecule carries only a very small amount of charge of 0.01e (as depicted in table S1 and figures S6(a), (b)) when it interacts with pristine AGNR at both edge and center doped configuration. There is no overlap exists between phosgene and pristine AGNR (figures S6(a), (b)) which indicates weak type of interaction.

Interaction of phosgene with 'B' atoms in B edge AGNR (figure S6(c)) and B center AGNR (figure S6(d)) transfers a charge of 0.03e and 0.02e towards phosgene molecule which is mainly obtained from the 'B' atom. When phosgene molecule interacts with the BP doped geometries, significant charge transfer takes place between the phosgene and BP doped geometries having values 003e and 0.08e for BP edge AGNR and BP center AGNR (figure S6(e),(f)). A small overlap exists between phosgene and B doped geometries (figure S6(c),(d)). Thus, the computational data of charge transfer is consistent with adsorption energy study.

To further understand the interaction mechanism between phosgene and 'P' doped AGNR, the charge density difference images are shown in figure 6. These images illustrated that an overlap between phosgene and P doped geometries indicating a strong covalent interaction between phosgene and P doped AGNR (edge/center). Figures 6(a), (b)) shows a large amount of charge transfer from P doped AGNR to phosgene having values are 0.07e and 0.08e for P edge AGNR and P center AGNR, respectively. These results of charge transfer are supported by data obtained from adsorption energy analysis.

4. Conclusion

In present work, the adsorption and electronic response of pristine as well as B/P/B+P doped armchair (AGNR) and zigzag (ZGNR) graphene nanoribbons towards phosgene molecule have been analyzed by DFT approach. The computational results reveal that pristine AGNR interacts with phosgene molecule via vander Waals forces of attraction with a very less negative value of E_{ads}. However P-doped systems demonstrated chemisorption and stronger sensitivity towards phosgene detection (more negative value of E_{ads}) and more charge gets transfer for this doping. We found that regardless of nanoribbon geometry, prominent binding energies for P-doped systems exhibit uniformity (within the range of −8.01 eV to −8.49 eV), displaying a slight negative correlation with nanoribbon width increase in both armchair and zigzag configurations; notably, adsorption energies in ZGNR are considerably lower than those in AGNR. Band structure study predicts that P doping into graphene nanoribbons results into a substantial improvement in phosgene detection which is confirmed by the emergence of extra energy levels in the valence and conduction band of graphene domain and large band gap change. The DOS analysis predicts that P- doping in graphene nanoribbon shows sharp and more intense peaks which is due to difference in electronegativities of 'C' and 'P' atoms. The calculated results of more negative E_{ads} and large band gap variations for P doped geometries show an increased sensitivity towards phosgene detection. These findings provide a useful insight to develop the novel chemical sensors for phosgene detection by using P-doping in graphene systems. In a nutshell, the ordered doping predicted to be a good strategy for improving the sensitivity of graphene towards phosgene molecule and leads to a significant increase of the adsorption energies.

Data availability statement

All data that support the findings of this study are either included within the article (and any supplementary files), or are available from the corresponding author upon reasonable request.

ORCID iDs

R Deji https://orcid.org/0000-0001-8322-0946
G N Nagy https://orcid.org/0000-0002-0416-4120
Ramesh K Sharma https://orcid.org/0000-0002-2637-1841
Manish K Kashyap https://orcid.org/0000-0001-5363-9842
Mousumi Upadhyay Kahaly https://orcid.org/0000-0002-8128-8397

References

[1] Donarelli M and Ottaviano L 2018 2D materials for gas sensing applications: a review on graphene oxide, MoS2, WS2 and phosphorene *Sensors* **18** 3638
[2] Fadardi M A and Movlarooy T 2023 Simulation of NO_x and CO_x gas sensor based on pristine armchair stanene nanoribbon *Advanced Theory and Simulations* **6** 2200875
[3] Hosseinian A, Salary M, Arshadi S, Vessally E and Edjlali L 2018 The interaction of phosgene gas with different BN nanocones: DFT studies *Solid State Commun.* **269** 23–7
[4] Borak J and Diller W F 2001 Phosgene exposure: mechanisms of injury and treatment strategies *J Occup Environ Med.* **43** 110–9
[5] Beheshtian J, Noei M, Soleymanabadi H and Peyghan A A 2013 Ammonia monitoring by carbon nitride nanotubes: a density functional study *Thin Solid Films* **534** 650–4
[6] Noei M, Ebrahimikia M, Saghapour Y, Khodaverdi M, Salari A A and Ahmadaghaei N 2015 Removal of ethyl acetylene toxic gas from environmental systems using AlN nanotube *Journal of Nanostructure in Chemistry* **5** 213–7
[7] Rezaei-Sameti M and Samadi Jamil E 2016 The adsorption of CO molecule on pristine, As, B, BAs doped (4, 4) armchair AlNNTs: a computational study *Journal of Nanostructure in Chemistry* **6** 197–205
[8] Attaran A M, Abdol-Manafi S, Javanbakht M and Enhessari M 2016 Voltammetric sensor based on Co_3O_4 /SnO_2 nanopowders for determination of diltiazem in tablets and biological fluids *Journal of Nanostructure in Chemistry* **6** 121–8
[9] Goodarzi Z, Maghrebi M, Zavareh A F, Mokhtari-Hosseini Z B, Ebrahimi Hoseinzadeh B, Zarmi A H and Barshan-Tashnizi M 2015 Evaluation of nicotine sensor based on copper nanoparticles and carbon nanotubes *Journal of Nanostructure in Chemistry* **5** 237–42
[10] Salih E, Mekawy M, Hassan R Y and El-Sherbiny I M 2016 Synthesis, characterization and electrochemical-sensor applications of zinc oxide/graphene oxide nanocomposite *Journal of Nanostructure in Chemistry* **6** 137–44
[11] Shokrieh M M, Saeedi A and Chitsazzadeh M 2013 Mechanical properties of multiwalled carbon nanotube/polyester nanocomposites *Journal of Nanostructure in Chemistry* **3** 1–5
[12] Kahaly M U and Waghmare U V 2007 Vibrational properties of single-wall carbon nanotubes: A first-principles study *Bull. Mater. Sci.* **31** 335–41
[13] Kahaly M U and Waghmare U V 2008 Effect of curvature on structures and vibrations of zigzag carbon nanotubes: A first-principles study *Bull. Mater. Sci.* **31** 335–41
[14] Upadhyay Kahaly M and Waghmare U V 2007 Size dependence of thermal properties of armchair carbon nanotubes: A first-principles study *Appl. Phys. Lett.* **91** 023112
[15] Fritea L, Banica F, Costea T O, Moldovan L, Dobjanschi L, Muresan M and Cavalu S 2021 Metal nanoparticles and carbon-based nanomaterials for improved performances of electrochemical (Bio) sensors with biomedical applications *Materials* **14** 6319
[16] Dinadayalane T C and Leszczynski J 2012 Fundamental structural, electronic, and chemical properties of carbon nanostructures: graphene, fullerenes, carbon nanotubes, and their derivatives *In Handbook of Computational Chemistry* 793–867(Springer)
[17] Upadhyay Kahaly M, Misra S and Mishra S K 2017 Photo-assisted electron emission from illuminated monolayer graphene *J. Appl. Phys.* **121** 205110
[18] Deji R, Verma A, Kaur N, Choudhary B C and Sharma R K 2022 Adsorption chemistry of co-doped graphene nanoribbon and its derivatives towards carbon based gases for gas sensing applications: Quantum DFT investigation *Mater. Sci. Semicond. Process.* **146** 106670
[19] Deji R, Jyoti R, Verma A, Choudhary B C and Sharma R K 2022 A Theoretical study of HCN adsorption and width effect on co-doped armchair Graphene Nanoribbon *Computational and Theoretical Chemistry* **1209** 113592
[20] Thakur J, Kashyap M K, Taya A, Rani P, Saini H S and Reshak A H 2017 Structure stability and magnetism in graphene impurity complexes with embedded V and Nb atoms *J. Magn. Magn. Mater.* **433** 109–15
[21] Singla R, Kumar S, Hackett T A, Reshak A H and Kashyap M K 2021 Genesis of magnetism in graphene/MoS2 van der Waals heterostructures via interface engineering using Cr-adsorption *J. Alloys Compd.* **859** 157776
[22] Felegari Z and Hamedani S 2017 Adsorption properties of the phosgene molecule on pristine graphyne, BN-and Si-doped graphynes: DFT study *Results in Physics* **7** 26262631
[23] Beheshtian J, Peyghan A A and Bagheri Z 2012 Detection of phosgene by Sc-doped BN nanotubes: a DFT study *Sensors Actuators B* **171** 846–52
[24] Srivastava P, Sharma V and Jaiswal N K 2015 $COCl_2$ gas adsorption on zigzag boron nitride nanoribbons: first principles study *Journal of Computational and Theoretical Nanoscience* **12** 2472–6
[25] Shakerzadeh E, Khodayar E and Noorizadeh S 2016 Theoretical assessment of phosgene adsorption behavior onto pristine, Al-and Ga-doped $B1_2N1_2$ and $B1_6N1_6$ nanoclusters *Comput. Mater. Sci.* **118** 155–71
[26] Baei M T, Soltani A, Hashemian S and Mohammadian H 2014 $Al_{12}N_{12}$ nanocage as a potential sensor for phosgene detection *Can. J. Chem.* **92** 605–10
[27] Zhang T, Sun H, Wang F, Zhang W, Tang S, Ma J and Zhang J 2017 Adsorption of phosgene molecule on the transition metal-doped graphene: First principles calculations *Appl. Surf. Sci.* **425** 340–50

[28] Manade M, Vines F and Illas F 2015 Transition metal adatoms on graphene: A systematic density functional study *Carbon* **95** 525–34
[29] Kahaly M U and Waghmare U V 2008 Contrast in the electronic and magnetic properties of doped carbon and boron nitride nanotubes: a first-principles study *The Journal of Physical Chemistry C* **112** 3464–72
[30] Kahaly M U 2009 Defect states in carbon nanotubes and related band structure engineering: A first-principles study *J. Appl. Phys.* **105** 024312
[31] Zhang J J, Ma J and Feng X 2023 Precision synthesis of boron-doped graphene nanoribbons: recent progress and perspectives *Macromol. Chem. Phys.* **224** 2200232
[32] Vo T H, Shekhirev M, Kunkel D A, Orange F, Guinel M J F, Enders A and Sinitskii A 2014 Bottom-up solution synthesis of narrow nitrogen-doped graphene nanoribbons *Chem. Commun.* **50** 4172–4
[33] Deji R, Jyoti R, Choudhary B C, Singh R and Sharma R K 2021 Enhanced sensitivity of graphene nanoribbon gas sensor for detection of oxides of nitrogen using boron and phosphorus co-doped system: a first principles study *Sens. Actuators, A* **331** 112897
[34] Mehla R and Singh S 2022 Phosphorus doped armchair graphene nanoribbon as a sensing platform of NH3 detection: A DFT investigation *Mater. Today Proc.* **48** 569–72
[35] Deji R, Choudhary B C and Sharma R K 2021 Novel hydrogen cyanide gas sensor: A simulation study of graphene nanoribbon doped with boron and phosphorus *Physica E* **134** 114844
[36] Liu J, Zhang Z H, Deng X Q, Fan Z Q and Tang G P 2015 Electronic structures and transport properties of armchair graphene nanoribbons by ordered doping *Org. Electron.* **18** 135–42
[37] Huang B, Li Z, Liu Z, Zhou G, Hao S, Wu J and Duan W 2008 Adsorption of gas molecules on graphene nanoribbons and its implication for nanoscale molecule sensor *The Journal of Physical Chemistry. C Nanomaterials and Interfaces* **112**
[38] Shekhirev M, Lipatov A, Torres A, Vorobeva N S, Harkleroad A, Lashkov A, Sysoev V and Sinitskii A 2020 Highly selective gas sensors based on graphene nanoribbons grown by chemical vapor deposition *ACS Appl. Mater. Interfaces* **12** 7392–402
[39] Hamann D R, Schlüter M and Chiang C 1979 Norm-conserving pseudopotentials *Phys. Rev. Lett.* **43** 1494
[40] Deji R, Verma A, Choudhary B C and Sharma R K 2022 New insights into NO adsorption on alkali metal and transition metal doped graphene nanoribbon surface: A DFT approach *J. Mol. Graphics Modell.* **111** 108109
[41] Kharwar S, Singh S and Jaiswal N K 2021 First-principle investigations of cove edged GaN nanoribbon for nanoscale resonant tunneling applications *Solid State Commun.* **340** 114486
[42] Mi T Y, Triet D M and Tien N T 2020 Adsorption of gas molecules on penta-graphene nanoribbon and its implication for nanoscale gas sensor *Physics Open* **2** 100014
[43] Leed E A, Sofo J O and Pantano C G 2005 Electronic structure calculations of physisorption and chemisorption on oxide glass surfaces *Physical Review B* **72** 155427
[44] Tang Y, Liu Z, Shen Z, Chen W, Ma D and Dai X 2017 Adsorption sensitivity of metal atom decorated bilayer graphene toward toxic gas molecules (CO, NO, SO_2 and HCN) *Sensors Actuators B* **238** 182–95
[45] Chang Z, Mebed A M, Mushtaq M, Ali H E, Muhammad I, Choudhary N and AlHosiny N M 2022 Adsorption, sensing, electronic and magnetic properties of phosgene ($COCl_2$) molecule adsorbed on Nb-doped arsenene: First-principles study *Solid State Commun.* **357** 114975
[46] Soliman K A and Aal S A 2022 Ti, Ni, and Cu decorated borospherene as potential molecular sensor for phosgene *Mater. Sci. Semicond. Process.* **144** 106574
[47] Klimchitskaya G L, Mostepanenko V M and Petrov V M 2017 Conductivity of graphene in the framework of Dirac model: Interplay between nonzero mass gap and chemical potential *Physical Review B* **96** 235432
[48] Kweitsu E O, Armoo S K, Kan-Dapaah K, Abavare E K K, Dodoo-Arhin D and Yaya A 2020 Comparative study of phosgene gas sensing using carbon and boron nitride nanomaterials-A DFT approach *Molecules (Basel, Switzerland)* **26** 120
[49] Salih E and Ayesh A I 2020 CO, CO_2, and SO_2 detection based on functionalized graphene nanoribbons: first principles study *Physica E* **123** 114220
[50] Bhuvaneswari R and Chandiramouli R 2019 First-principles investigation on detection of phosgene gas molecules using phosphorene nanosheet device *Chem. Phys. Lett.* **717** 99–106